Design of Radial Inflow Turbine for 30 kW Microturbine

Thanate Sangsawangmatum and Udomkiat Nontakaew

Faculty of Engineering, Department of Mechanical and Aerospace Engineering, KMUTNB, Thailand

Abstract. Microturbines are small gas turbines that have the capacity range of 25-300 kW. The main components of microturbine are compressor, turbine, combustor and recuperator. This research paper focuses on the design of radial inflow turbine that operates in 30 kW microturbine. In order to operate the 30 kW microturbine with the back work ratio of 0.5, the radial inflow turbine should be designed to produce power at 60 kW. With the help of theory of turbo-machinery and the analytical methods, the design parameters are derived. The design results are constructed in 3D geometry. The 3D fluid-geometry is validated by computational fluid dynamics (CFD) simulation. The simulation results show the airflow path, the temperature distribution, the pressure distribution and Mach number. According to the simulation results, there is no flow blockage between vanes and no shock flow occurs in the designed turbine.

1 Introduction

Microturbines are small gas turbines that have the capacity range of 25-300 kW. They offer several advantages compared to other technologies including compact size, small number of moving parts, low emissions and lead to opportunities to utilize waste fuels. [1]

The main components of microturbine are compressor, turbine, combustor and recuperator. This research paper focuses on the 30 kW microturbine with an operating speed is about 40,000 rpm. The design and analysis of a radial inflow turbine that is a specific kind of turbine is suitable for microturbine application. In order to investigate the appropriate geometry of radial inflow turbine for 30 kW microturbine applications, the theory of turbo machinery is applied and the analytical design result is validated by the methods of computational fluid dynamics (CFD).

The method of computational fluid dynamics (CFD) is a branch of fluid mechanics that applies numerical analysis and algorithm to analyse the fluid flow problem and has been widely used in several research papers as shown [2]. This research paper analyses an intermediate pressure steam turbine using CFD. The domain of the steam turbine bladed region is modelled discretized in three zones; stationary blades, moving blades and labyrinth seals, and governing equations are solved. The CFD results show the pressure contour plot for each stage. It can be seen that the method of computational fluid dynamics is very useful for visualize and understanding the flow in the domain of complex geometries.

The ideal cycle, Brayton cycle, for 30 kW microturbine is shown in Fig. 1.

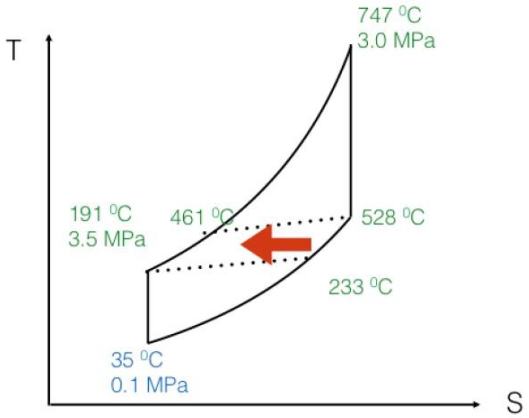

Figure 1. The Brayton cycle for 30 kW microturbine.

The assumptions of ideal conditions made in the design process are as follows: The compression and expansion processes are adiabatic reversible or isentropic. The changes of kinetic energy of the working fluid between inlet and outlet of each component are neglect. There are no pressure losses in the inlet ducting, combustion chambers, heat exchangers, exhaust ducting, and ducts connecting the components.

The working fluid has the same composition throughout the cycle and is a perfect gas with constant specific heats. The mass flow rate of gas is constant throughout the cycle. Heat transfer in a counterflow heat exchanger (recuperator) is complete so that the temperature rise on the cold side is the maximum as possible and can be considered as exactly equal to the temperature drop on the hot side.

2 Radial inflow turbine design process

The radial-inflow turbine stage geometry is illustrated in [3]. The flow enters the stage through an inlet volute and the flow area is constant in the circumferential direction before passes through a vaneless annular passage into a nozzle blade row.

The flow passes through another vaneless annular passage to enter the rotor row. An exhaust diffuser is next after the rotor row to convert some of the rotor exit velocity to static pressure. Hence, the basic stage components to be analysed are the inlet volute, nozzle, rotor, and vaneless annular passages and exhaust diffuser. In this research paper, the radial-inflow turbines to be analysed are single-stage units. The theoretical analysis and studies of the boundary layer, the boundary layer loss coefficient, the inlet volute, the nozzle row, the rotor, the vaneless annular passage, and the exhaust diffuser are also summarized. The basic analysis for each stage of radial flow turbines is performed in [4] and [5].

In the radial inflow turbine design process, air is considered as the working fluid with a flow rate of 0.28 kg/s. Turbine inlet temperature and turbine inlet pressure are 747 K and 3 bar, respectively.

The specific speed (N_s) and the specific diameter (D_s) can be calculated as

$$N_s = N\,(Q_3)^{1/2} / (\Delta H_{ad})^{3/4} \quad (1)$$

$$D_s = D\,(\Delta H_{ad})^{1/4} / (Q_3)^{1/2} \quad (2)$$

where N is the impeller rotation speed (rpm), Q_3 is the turbine exhaust air flow rate (m^3/s), ΔH_{ad} is an isentropic head expand in turbine (m) and D is the diameter of the impeller (m). The air velocity equivalent to the isentropic enthalpy drop, c_o , can be calculated as, see Fig. 2,

$$c_o = \{2C_p\,[T_{o1} - T_{o3}]\}^{1/2} \quad (3)$$

where C_p is the specific heat at constant pressure (kJ/kg·K), T_{o1} is the stagnation temperature at turbine inlet (K), γ is the pressure ratio and k is the ratio of specific heat at constant pressure and specific heat at constant volume and is equal to a constant of 1.4.

Substitute the value of C_p, T_{o1}, γ and k into equation (3), the air velocity which is equivalent to the isentropic enthalpy drop, c_o ,can be calculated as

$$c_o = \{2(1004)[722 - 528]\}^{1/2} = 624\ m/s \quad (4)$$

According to the previous researches and studies, the best efficiency point of radial inflow turbine can be determined by the quotient of the air velocity at the turbine outlet (U_2) to the velocity which equivalent to the isentropic enthalpy drop (c_o) and is found between 0.68 and 0.71.

$$0.68 < U_2/c_o < 0.71 \quad (4)$$

Turbine mass flow rate is equal to 0.32 m^3/s. Gas density at the exit condition is equal to 0.44 kg/m^3. The volume flow rate at the turbine exit can be determined as

$$Q_3 = 0.32 / 0.44 = 0.73\ m^3/s = 25.78\ ft^3/s$$

$$W = h_{01} - h_{03} = C_p\,(T_{01} - T_{03}) \quad (5)$$

$$H_{ad} = W / g = C_p\,(T_{01} - T_{03})/g \quad (6)$$

$$H_{ad} = 1004(722\text{-}528)/9.81 = 19{,}854.84\ m$$

$$= 65{,}140.55\ ft$$

From equation (1),

$$N_s = 47{,}000\,(15.78)^{1/2} / (65{,}140.55)^{3/4} \quad (7)$$

$$N_s = 58.53$$

According to the specific speed chart, the specific diameter is equal to 1.8. Then

$$D = D_s\,(Q_3)^{1/2} / (\Delta H_{ad})^{1/4}$$

$$D = 1.8\,(25.78)^{1/2} / (65{,}140.55)^{1/4}$$

$$D = 0.57\ ft = 174\ mm.$$

$$U = \prod ND/60 \quad (8)$$

$$U = \prod \cdot 47{,}000 \cdot 174 / (60 \cdot 1000) = 427.98\ m/s$$

From S.L.Dixon, the optimum ratios of the tip diameter to the turbine diameter and the hub diameter to the tip diameter for microturbine are

$$D_t/D_2 < 0.7 \quad and \quad D_h/D_t > 0.35 \quad (9)$$

This research paper uses

$$D_t/D_2 = 0.65 \quad and \quad D_h/D_t = 0.35$$

Therefore, the D_t and D_h are equal to 113.1 mm and 40 mm, respectively.

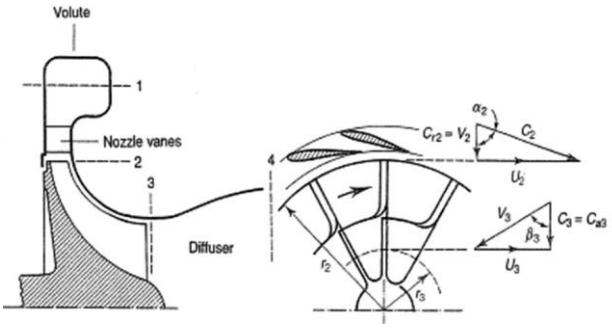

Figure 2. Turbine velocity diagram.

Assume that the outlet gas flows are uniform,

$$U_{3,mean} = (2\prod N/60)\, r_{3,mean} \quad (10)$$

$$U_{3,mean} = (2 \cdot \prod \cdot 47{,}000/60) \cdot 38.25/1000 = 188.65\ m/s$$

The turbine outlet area are then calculated, the blade thickness is negligible,

$$A_3 = \prod (D_h^2 - D_t^2)/4 = 8.77x10^{-3}\ m^2$$

The axial outlet gas velocity are calculated as

$$C_3 = Q_3 / A_3 = 0.73 / (8.77x10^{-3}) = 83.26\ m/s$$

Then the rotor outlet angle ($ß_{2,mean}$) can be calculated as

$$ß_{3,mean} = tan^{-1} (U_{3,mean} / C_3) = tan^{-1} (188.65 / 83.26) = 66.19°$$

3 Computational fluid dynamics (CFD)

The control volume is separated into two parts with the interface surface is between. The first part is a stationery part: the nozzle vane, as shown in Fig. 3. This nozzle vane composed of 11 air foils NACA with an exit angle of 58°.

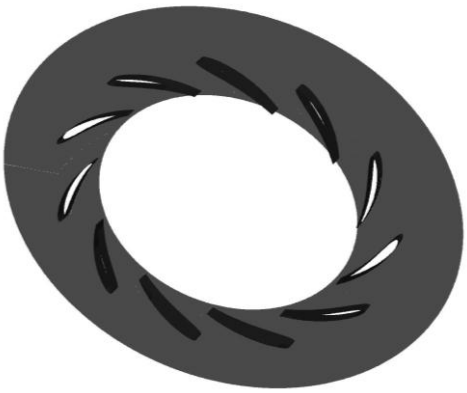

Figure 3. Computational domain of the nozzle vane.

The second part is a moving part: the turbine impeller, as shown in Fig. 4. The designed parameter is based on the value from the previous section. The turbine impeller is also composed of 11 blades. With the reason of the strength of material, the blade thickness at the hub and the tip are designed to be equal to 5 mm and 2 mm, respectively.

Figure 4. Computational domain of turbine impeller.

Fig. 5 shows the computational grid of both two zones. Each grid is in a shape of tetrahedral grid and hexahedral grid in the near wall area (the boundary zone). The computational domain of nozzle vane is divided into 226,923 elements and the computational turbine impeller is divided into 327,076 elements. The grid independent process ensure that the number of grid in both two domains are appropriate.

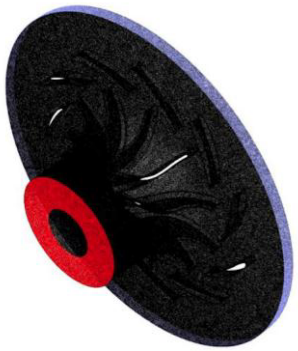

Figure 5. Computational grid.

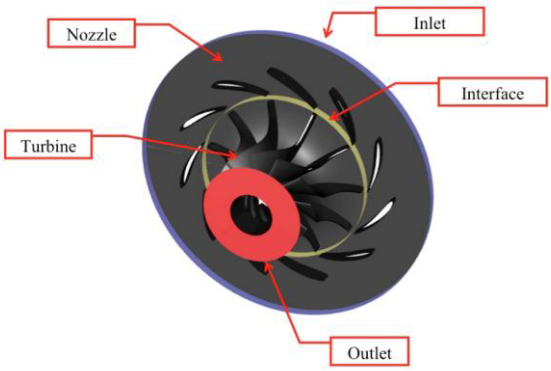

Figure 6. Boundary condition.

The boundary condition surface, Fig. 6, for numerical method is set up as shown in table 1 and the physical set up is shown in Table 2.

Table 1. Boundary condition setup

Position	Boundary condition
Inlet	Pressure ratio = 3 and 747ºc
Outlet	Pressure outlet at 0.5 bars and 528ºc
Blade and hub	Wall sliding mesh at 47,000 rpm, adiabatic wall
Nozzle	Stationary wall, adiabatic wall
Side shroud	Stationary wall, adiabatic wall

Table 2. Physical setup

Solver setting	Pressure-based
Discretization	Monotone upstream – Centered schemes for conservation law (MUSCL)
Interpolation methods	Green-Gauss Node-Based
Interpolation methods for face pressure	PRESTO
Pressure velocity coupling	Pressure-Implicit with splitting of operators (PISO)
Convergence residuals	Continuity equation = 10^{-5} Momentum equation = 10^{-5} Energy equation = 10^{-7}

4 Results and Discussions

The numerical solution from a time-dependent calculation at the time step is equal to $1x10^{-6}$ sec. The residual solution for continuity and momentum equation are below 10^{-5} and for the energy equation is below 10^{-7}. Flow time is equal to 0.01 sec. The solutions obtained from the numerical method are presents as shown in Fig. 7 to Fig. 11.

Fig. 7 shows the variation of air density. The maximum density occurs at the inlet and gradually decreases from the inlet to the outlet. Figure 8 shows that the Mach number is below the supersonic flow where the physical properties of fluid are rapidly changes. In other words, the flow is acceptable.

The pressure distribution, in Fig. 9, is corresponding to the density distribution. The maximum pressure occurs at the inlet. The temperature is about 540ºc at the outlet. The specified temperature at the inlet and outlet are distributed as shown in figure 10. It can be seen that there is no heat accumulate within the domain. From the above CFD results, there is no unusual phenomenon. The airflow path in Fig. 11 emphasize that there is no separation flow in the nozzle blade and impeller blade which is the main reason of the flow to be blocked and also decrease the flow channel. This leads to the decrease of mass flow rate and turbine efficiency.

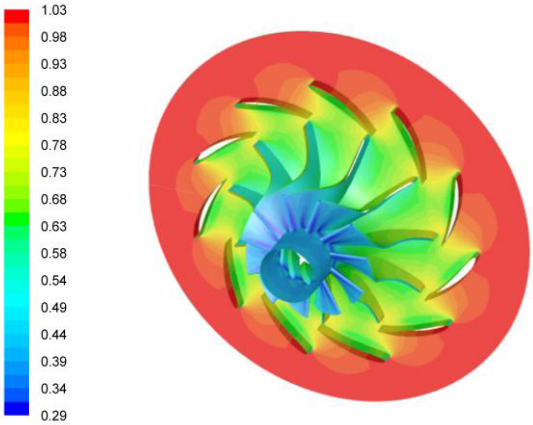

Figure 7. Density distribution.

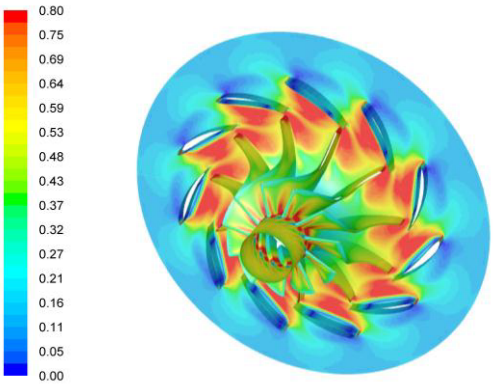

Figure 8. Mach number.

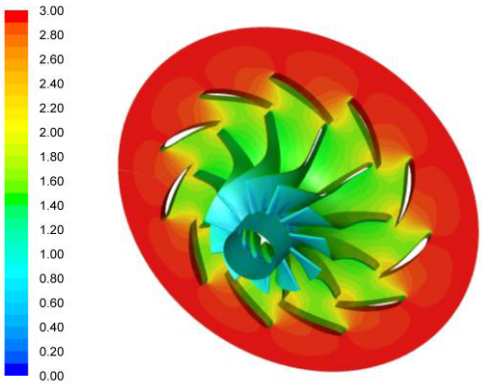

Figure 9. Pressure distribution.

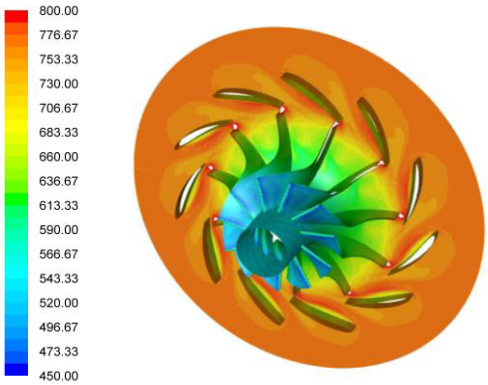

Figure 10. Temperature distribution.

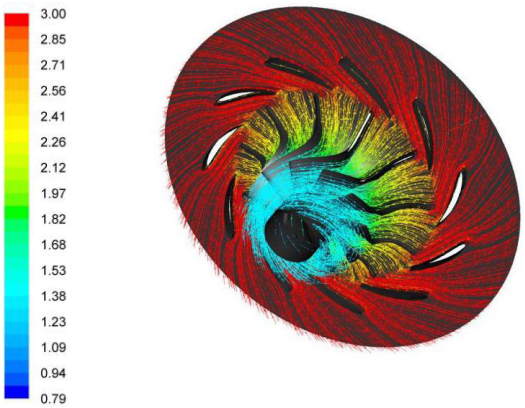

Figure 11. Air flow path depend on pressure.

5 Conclusions

This research paper focuses on the design of radial inflow turbine that operates in 30 kW microturbine. In order to operate the 30 kW microturbine with the back work ratio of 0.5, the radial inflow turbine should be designed to produce power at 60 kW. The radial inflow turbine is designed based on the turbo machinery theory. With the help of the analytical methods, the design parameters are derived. The results are constructed in 3D geometry and the 3D fluid-geometry is validated by computational fluid dynamics (CFD) simulation.

According to the CFD investigation, it shows that the temperature distribution and the pressure distribution at

the surface of the nozzle and turbine impeller are simultaneous. The simulation results also show the smoothness of the airflow path in the designed radial inflow turbine.

As can be seen from the figures, there is no flow blockage between vanes. The Mach number value is between 0 and 0.8, which is acceptable. This means that there is no shock flow occurs. In an engineering point of view, it can be concluded that the designed radial inflow turbine works well with the 30 kW microturbine.

References

1. C.F. McDonald, Applied Thermal Engineering, Vol.20(2000) 471-497.
2. S.Vasmate, Int.J.Mech.Eng.& Rob, Vol.3, No.4 (2014)
3. R.H. Aungier, Turbine Aerodynamics: Axial-Flow and Radial-Inflow Turbine Design and Analysis (ASME Press, 2006)
4. D. Japikse and N.C.Baines. Introduction to Turbomachinery (Oxford University Press, 1994)
5. S.L.Dixon. Fluid Mechanics, Thermodynamics of Turbomachinery (Pergamon Press, 1978)